Charged particle multiplicity in Pb-Pb collisions from the NA50 experiment

Francesco Prino[11] **for the NA50 collaboration**
B Alessandro[11], **C Alexa**[4], **R Arnaldi**[11], **M Atayan**[13], **C Baglin**[2], **A Baldit**[3], **M Bedjidian**[12], **S Beolè**[11], **V Boldea**[4], **P Bordalo**[7,a], **S R Borenstein**[10,b], **G Borges**[7], **A Bussière**[2], **L Capelli**[12], **C Castanier**[3], **J Castor**[3], **B Chaurand**[10], **B Cheynis**[12], **E Chiavassa**[11], **C Cicalò**[5], **T Claudino**[7], **M P Comets**[9], **S Constantinescu**[4], **P Cortese**[1], **J Cruz**[7], **A DeFalco**[5], **N DeMarco**[11], **G Dellacasa**[1], **A Devaux**[3], **S Dita**[4], **O Drapier**[10], **B Espagnon**[3], **J Fargeix**[3], **P Force**[3], **M Gallio**[11], **Y K Gavrilov**[8], **C Gerschel**[9], **P Giubellino**[11,c], **M B Golubeva**[8], **M Gonin**[10], **A A Grigorian**[13], **S Grigorian**[13], **J Y Grossiord**[12], **F F Guber**[8], **A Guichard**[12], **H Gulkanyan**[13], **R Hakobyan**[13], **R Haroutunian**[12], **M Idzik**[11,d], **D Jouan**[9], **T L Karavitcheva**[8], **L Kluberg**[10], **A B Kurepin**[8], **Y Le Bornec**[9], **C Lourenço**[6], **P Macciotta**[5], **M Mac Cormick**[9], **A Marzari-Chiesa**[11], **M Masera**[11], **A Masoni**[5], **M Monteno**[11], **A Musso**[11], **P Petiau**[10], **A Piccotti**[11], **J R Pizzi**[12], **W L Prado da Silva**[11,e], **F Prino**[11], **G Puddu**[5], **C Quintans**[7], **L Ramello**[1], **S Ramos**[7,a], **P Rato Mendes**[7], **L Riccati**[11], **A Romana**[10], **H Santos**[7], **P Saturnini**[3], **E Scalas**[1] **E Scomparin**[11], **S Serci**[5], **R Shahoyan**[7,f], **F Sigaudo**[11], **M Sitta**[1], **P Sonderegger**[6,a], **X Tarrago**[9], **N S Topilskaya**[8], **G L Usai**[5], **E Vercellin**[11], **L Villatte**[9], **N Willis**[9] **and T Wu**[9]

[1] Università del Piemonte Orientale, Alessandria and INFN-Torino, Italy;
[2] LAPP, CNRS-IN2P3, Annecy-le-Vieux, France;
[3] LPC, Univ. Blaise Pascal and CNRS-IN2P3, Aubière, France;
[4] IFA, Bucharest, Romania;
[5] Università di Cagliari/INFN, Cagliari, Italy;
[6] CERN, Geneva, Switzerland;
[7] LIP, Lisbon, Portugal;
[8] INR, Moscow, Russia;
[9] IPN, Univ. de Paris-Sud and CNRS-IN2P3, Orsay, France;
[10] Laboratoire Leprince-Ringuet, Ecole Polytechnique and CNRS-IN2P3, Palaiseau, France;
[11] Università di Torino/INFN, Torino, Italy;
[12] IPN, Univ. Claude Bernard Lyon-I and CNRS-IN2P3, Villeurbanne, France;
[13] YerPhI, Yerevan, Armenia.
a) also at IST, Universidade Técnica de Lisboa, Lisbon, Portugal; b) on leave of absence from York College, CUNY, New York, USA; c) also at CERN, Geneva, Switzerland; d) also at Faculty of Physics and Nuclear Techniques, UMM, Cracow, Poland; e) now at UERJ, Rio de Janeiro, Brazil; f) on leave of absence from YerPhI, Yerevan, Armenia.

E-mail: `prino@to.infn.it`

Abstract. Angular distributions of charged particles produced in Pb-Pb collisions at the CERN SPS have been measured by the NA50 experiment. Measurements have been performed with a silicon microstrip detector at two different beam energies (40 and 158 GeV/nucleon) and over a wide impact parameter (centrality) range. The centrality of the collision has been evaluated both by neutral transverse energy released in the interaction and by spectator nucleons energy (zero degree energy).

The charged particle density at midrapidity shows a linear dependence on the number of participating nucleons at both beam energies. The particle density per participant pair and its $\sqrt{s}$ dependence are also studied.

1. Introduction

The multiplicity detector of the NA50 experiment, with its good granularity, allows to measure the angular distribution of the charged particles produced in Pb–Pb collisions at the CERN SPS, providing the pseudorapidity distributions of charged particles ($dN_{\mathrm{ch}}/d\eta$) over a wide η range [1]. The multiplicity of charged particles produced in the collisions is a global variable that is essential for their characterization, because it quantifies to which extent the incoming beam energy is released to produce new particles. Furthermore, the particle density at midrapidity ($dN/d\eta\ |_{\mathrm{max}}$) gives information about initial conditions of the collision evolution, such as the energy density.

The pseudorapidity distributions of primary charged particles have been measured for different classes of events selected according to the centrality of the collision. Two analyses have been performed using two independent centrality-related observables: the energy of the projectile spectator nucleons measured by a Zero Degree Calorimeter (E_{ZDC}) and the neutral transverse energy (E_{T}) measured by an Electromagnetic Calorimeter. In both cases, the centrality selection has been made using observables which are independent of the multiplicity detector itself, in order to avoid autocorrelations. The measurement of charged particle multiplicity as a function of centrality may help constrain different models of particle production, and quantify the relative importance of soft versus hard processes in the particle production mechanism at different energies. In this respect, an important test for models of particle production in heavy ion reactions is the study of its scaling properties with respect both to the number of participant nucleons (N_{part}) and to the number of binary collisions (N_{coll}).

Additional information relevant for constraining particle production models is provided by studying the scaling of charged particle multiplicity versus $\sqrt{s}$ compared to the one observed in nucleon-nucleon collisions. In order to enrich the pattern outlined by the results obtained at the AGS, SPS and RHIC, pseudorapidity distributions have been measured by the NA50 experiment at two different SPS Pb beam energies, namely 40 and 158 GeV per nucleon, corresponding to $\sqrt{s} = 8.77$ and 17.3 GeV respectively.

2. Experimental setup

The NA50 apparatus [2] consists of a muon spectrometer equipped with three detectors which measure centrality related observables on an event-by-event basis (namely charged particle multiplicity, neutral transverse energy and forward energy) and specific devices for beam tagging and interaction vertex identification. The present analysis uses data measured by the centrality detectors, as shown in figure 1.

The multiplicity and the angular distribution of charged particles are measured in a wide acceptance window by a Multiplicity Detector composed of two identical planes (MD1 and MD2) of silicon strip detectors [4, 5].

The determination of the centrality of the collision is obtained by means of a Zero Degree Calorimeter (ZDC) which measures the energy E_{ZDC} of the spectator nucleons traveling in the forward direction and by an electromagnetic calorimeter which measures the neutral transverse energy E_{T} in the pseudorapidity range $1.1 < \eta < 2.3$.

The analyzed data were collected in special runs taken at low beam intensity (about 1/10 of the standard intensity used by the experiment) with the Minimum Bias trigger, which requires a non-zero energy deposit in the ZDC.

3. Centrality selection and model calculations

The aim of our analysis is to study the properties of $dN_{\mathrm{ch}}/d\eta$ distributions in Pb–Pb collisions as a function of centrality using two independent centrality estimators, namely the forward energy E_{ZDC} and the transverse energy E_{T}. To allow a comparison of the results obtained with these two different variables, centrality intervals have been defined in terms of fractions

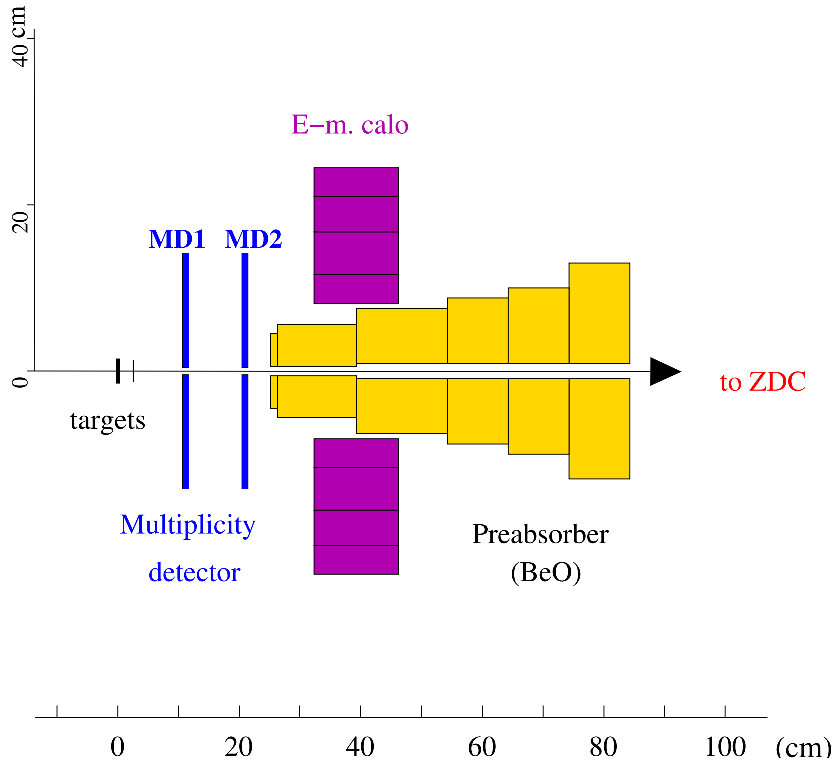

Figure 1. 1998 experimental setup.

of the inelastic cross section, which was calculated by integrating the dN/dE_{ZDC} and dN/dE_{T} distributions of the events collected with the Minimum Bias trigger. The contribution of non-interacting projectiles which fire the Minimum Bias trigger is removed by taking into account the Pb–Pb interaction probability, calculated as explained in [1].

The limits of each centrality class have been fixed so as to have classes with a width corresponding to 5% of the total inelastic cross section σ_{inel}. When the 5% class would have been too narrow with respect to the E_{ZDC} or E_{T} resolution thus giving rise to possible biases in the centrality selection, a class with a width corresponding to $10\%{\cdot}\sigma_{\mathrm{inel}}$ has been defined. In this way, six centrality classes have been defined for both centrality estimators. For the data sample collected at 40 GeV per nucleon incident energy, due to the worse performance of the ZDC at such a low beam energy, it was not possible to use both centrality estimators and only the analysis with the E_{T} based centrality selection has been performed.

For each centrality class, the average values of N_{part} and N_{coll} have been estimated in the framework of the Glauber model assuming that E_{T} is proportional to the number of participants and E_{ZDC} to the number of projectile spectators. Smearing effects due to the experimental resolution of the calorimeters have also been included in our calculation. In figure 2 we show a comparison between the E_{T} and E_{ZDC} Minimum Bias spectra calculated with the Glauber model and the experimentally measured ones with and without the vertex constraint. The vertex constraint is based on the geometrical correlation between the hits on the two MD planes and rejects the non interacting Pb ions whose contribution dominates the spectra at high E_{ZDC}-low E_{T}. The E_{ZDC} and E_{T} limits for the different centrality classes can be found in [1], while the results concerning N_{part} and N_{coll} are reported in [3].

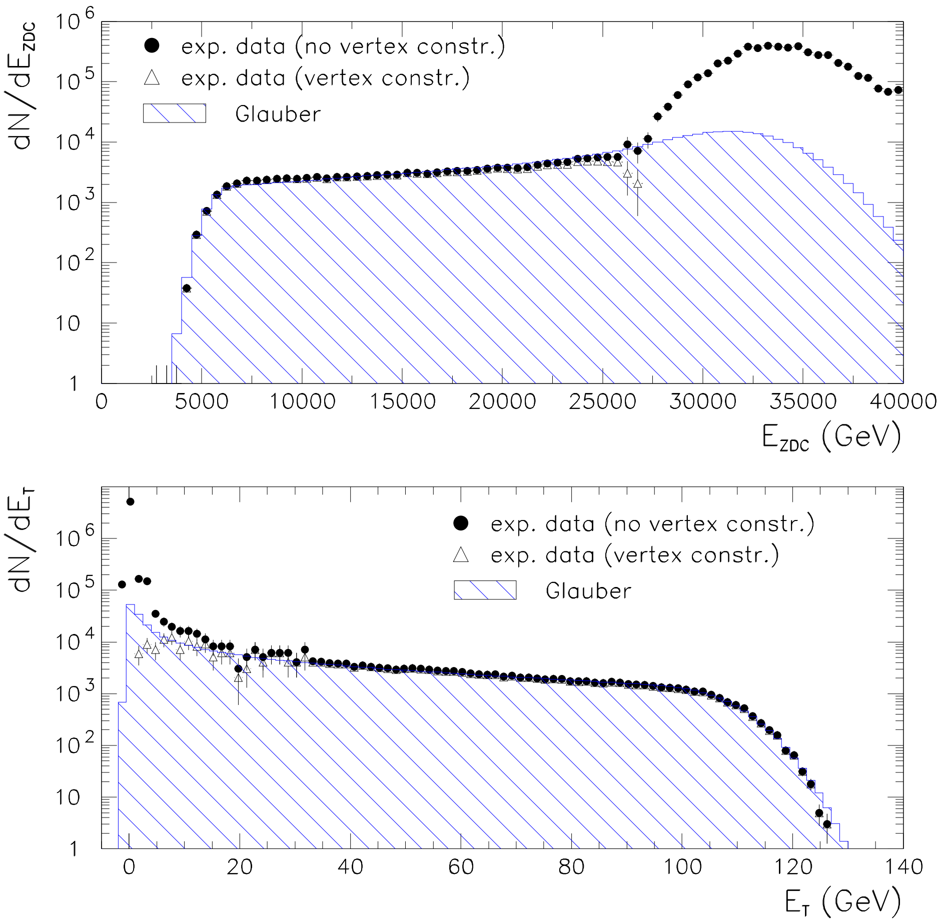

Figure 2. Distributions of the forward energy E_{ZDC} and of the neutral transverse energy E_T in Pb–Pb collisions at 158 GeV per nucleon incident energy. Predictions of the Glauber model are superimposed (hatched histograms).

4. Data analysis

The data analysis has been performed in each centrality class, according to the following procedure. First some quality cuts ensuring rejection of beam pile–up and out of target interactions have been applied on the data sample. Then in each centrality class the raw $dN_{\rm ch}/d\eta$ distribution has been calculated from the multiplicity detector occupancy after correcting for geometrical (one particle crossing 2 or more contiguous strips) and instrumental (such as crosstalk between electronic channels) effects. Finally, the primary $dN_{\rm ch}/d\eta$ distribution has been obtained by subtracting the delta electron contribution and then by correcting for secondary processes. Gamma conversions and other processes of secondary particle production or primary particle decay have been evaluated with a complete Monte Carlo simulation based on the VENUS 4.12 event generator and on the GEANT 3.21 package for track propagation and detector response simulation. The δ ray contribution to the detector occupancy is evaluated by means of a GEANT 3.21 simulation and it reaches a maximum of 5% of the true occupancy, in the most peripheral sample considered in this paper.

The resulting $dN_{\rm ch}/d\eta$ particle distributions from MD1 and MD2, being in agreement in their common η range, are then merged together, providing a wider η coverage. As a final check, the complete procedure is applied to two data samples with different target thickness and position, obtaining results in good agrement between them.

We estimate the overall systematic error on the evaluated multiplicity to be below 8%. For the 40 GeV/nucleon data, since only $E_{\rm T}$ is used as centrality estimator, a larger systematic error (10%) is estimated. More details can be found in [1].

5. Results

5.1. Pseudorapidity distributions at 158 GeV/nucleon

The pseudorapidity distributions of primary charged particles obtained at 158 GeV/nucleon beam energy using $E_{\rm ZDC}$ and $E_{\rm T}$ as centrality estimators are shown in figure 3. The pseudorapidity coverage is approximately centered at midrapidity and extends over ~ 2.2 units, so that the $dN_{\rm ch}/d\eta$ peak is visible in the pseudorapidity distributions without any reflection around midrapidity. The $dN_{\rm ch}/d\eta$ distributions are rather symmetrical around the midrapidity point. The pseudorapidity distributions thus obtained have been fitted with Gaussian functions, to obtain an estimate of the charged particle pseudorapidity density at the peak ($dN/d\eta\ |_{\rm max}$), of the peak position ($\eta_{\rm max}$) and of the gaussian width (σ_η).

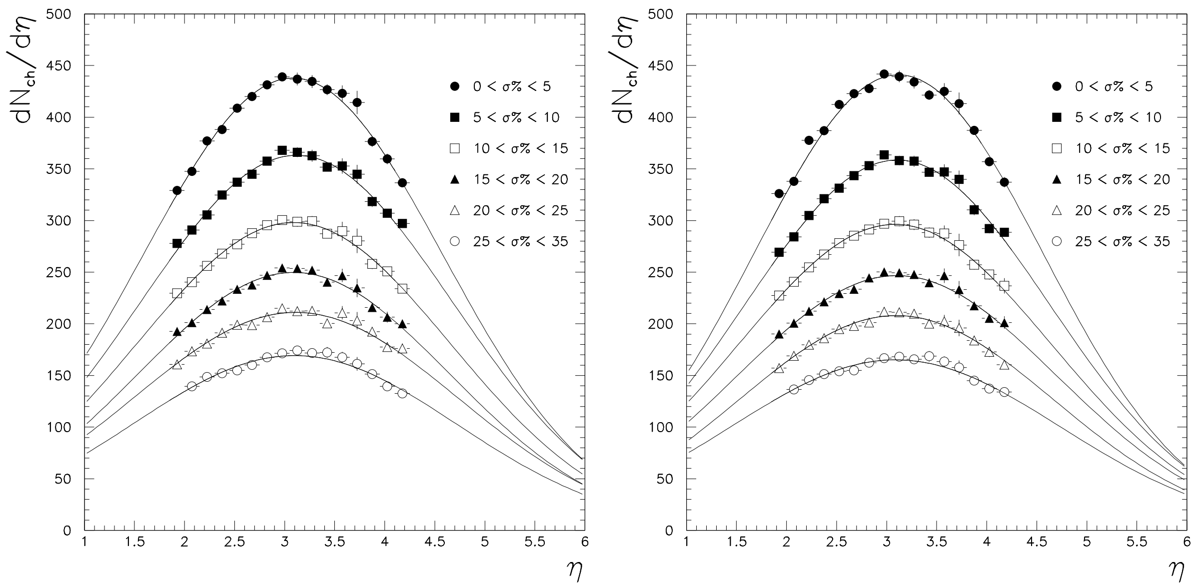

Figure 3. Pseudorapidity distributions of charged particles in 158 GeV/nucleon Pb–Pb collisions obtained using $E_{\rm ZDC}$ (left) and $E_{\rm T}$ (right) as centrality estimators. Gaussian fits are superimposed.

The results obtained with the two independent centrality estimators are in agreement within 1.5% except for the most peripheral class where the difference between the $dN/d\eta\ |_{\rm max}$ values amount to $\simeq$2.5%. The midrapidity values resulting from the Gaussian fits are compatible with the value $\eta_{\rm max}\simeq 3.1$ extracted from VENUS and corresponding to $y_{\rm max}$=2.91. The width of the gaussian fits to $dN_{\rm ch}/d\eta$ distributions for both centrality estimators ($\sigma_\eta \simeq 1.5 - 1.6$) show a decrease of $\approx$ 10% when going from our most peripheral class to our most central one. The narrowing of the shape of pseudorapidity distributions with increasing centrality, observed by several other experiments, can be associated with the higher degree of stopping reached in the interaction, and it is mostly due to the decreasing contribution of protons from target and projectile fragmentation. It is also interesting to note that at 158 GeV/nucleon the width of the rapidity distributions is about twice as large as the one expected from a single thermal source located at midrapidity [6].

The particle density at midrapidity ($dN/d\eta\,|_{\rm max}$) increases steadily with increasing centrality showing an approximately linear dependence of the charged multiplicity on both $E_{\rm T}$ and $E_{\rm ZDC}$ (for more details see [1]).

5.2. Pseudorapidity distributions at 40 GeV/nucleon

In figure 4, the particle pseudorapidity distributions obtained for the data collected at 40 GeV per nucleon beam energy are shown as well as the results of Gaussian fits.

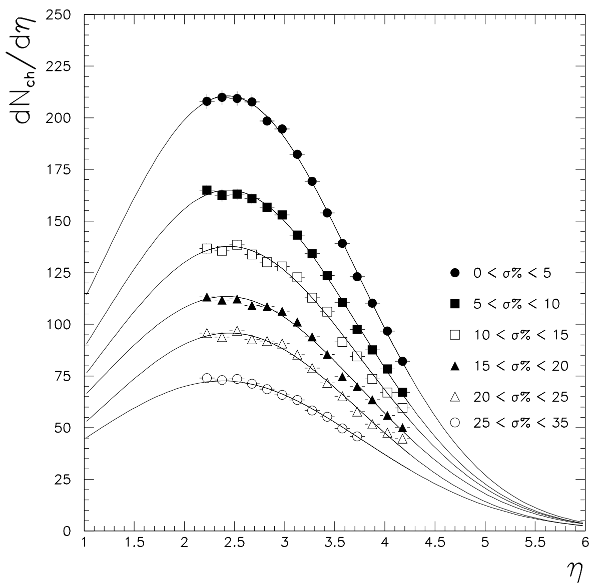

Figure 4. Pseudorapidity distributions of charged particles in 40 GeV/nucleon Pb–Pb collisions obtained using $E_{\rm T}$ as centrality estimator.

The $\eta_{\rm max}$ value expected from VENUS is 2.47 and is compatible with fit results. The width of the Gaussian fit to the pseudorapidity distributions ($\sigma_\eta \simeq 1.3 - 1.4$) shows the same centrality dependence (decreasing with increasing centrality) as the one observed at 158 GeV/nucleon. The gaussian width σ_η is lower than at 158 GeV/nucleon, reflecting the fact that the available phase space in rapidity increases with the center-of-mass energy. This result confirms the already observed fact that the width of the pseudorapidity distribution in central ion-ion collisions at AGS-SPS energies appears to follow a simple logarithmic scaling law independent of system size, for more details see [3]. The charged particle density at midrapidity ($dN/d\eta\,|_{\rm max}$) scales linearly as a function of $E_{\rm T}$. For the most central class it is approximately half the value measured at 158 GeV per nucleon.

5.3. Centrality dependence of charged particle production

To evaluate the centrality dependence of particle production, the scaling behaviour of the $dN/d\eta\,|_{\rm max}$ as a function of the number of participant nucleons $N_{\rm part}$ has been parametrized with the usual power law behaviour:

$$\left(\frac{dN_{\rm ch}}{d\eta}\right)_{\rm max} \propto N_{\rm part}^{\alpha}$$

The fit has been performed with the technique explained in [7] to take into account also the error on the independent variable $N_{\rm part}$. The value of the scaling exponent for the 158 GeV/nucleon data sample results to be $\alpha = 1.00 \pm 0.01(stat) \pm 0.04(syst)$ with both the $E_{\rm T}$ and the $E_{\rm ZDC}$ centrality selections, as it can be seen in figure 5. This value of α is in agreement with the Wounded Nucleon Model assumption that the average multiplicity in a collision is proportional to the number of participant (wounded) nucleons.

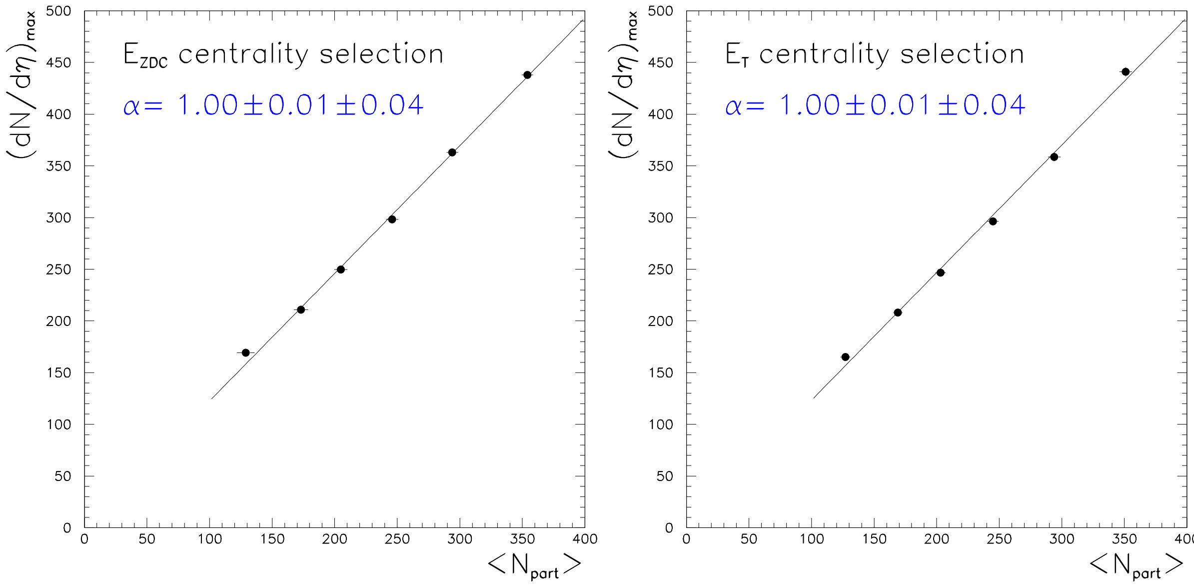

Figure 5. Pseudorapidity density of $N_{\rm ch}$ at midrapidity as a function of the number of participants in 158 GeV per nucleon Pb–Pb collisions with the two independent centrality selections. Power-law fits are superimposed.

It has to be stressed that the value of the exponent α is strongly dependent on the value of $N_{\rm part}$ and may vary significantly as a consequence of slight variations of $N_{\rm part}$. For this reason we performed also power law fits using different $< N_{part} >$ evaluations. If the values of $N_{\rm part}$ from VENUS 4.12 are used, we obtain $\alpha = 1.08$ with the $E_{\rm T}$ centrality selection and $\alpha = 1.05$ with the $E_{\rm ZDC}$ selection. For the $E_{\rm ZDC}$ centrality selection we performed also a fit using a straightforward $N_{\rm part}$ evaluation, namely $< N_{\rm part} >= 2 \cdot 208 \cdot (1 - E_{\rm ZDC}/E_{\rm beam})$, for which we obtain $\alpha = 1.02$.

A fit to the power law $dN/d\eta\ |_{\rm max} \propto\ {N_{\rm coll}}^{\beta}$ has also been performed, obtaining for the exponent the values $\beta = 0.74$ and $\beta = 0.76$ with $E_{\rm ZDC}$ and $E_{\rm T}$ centrality selections, respectively. Therefore, we can conclude that $N_{\rm part}$ is well suited to describe the scaling of particle production with the centrality of the collision and that a scaling like $N_{\rm coll}$ is not observed at this energy.

Finally, a fit with the function $dN/d\eta\ |_{\rm max} = A \times N_{\rm part} + B \times N_{\rm coll}$ has been done, in order to verify the possible presence of a term proportional to the number of collisions. The results of the fits for both centrality selections lead to values of B compatible with zero, indicating that the contribution from hard processes to charged particle production is negligible at this energy.

The data sample collected at 40 GeV per nucleon has also been fitted with ${N_{\rm part}}^{\alpha}$, using the Glauber calculation of $N_{\rm part}$. The value $\alpha = 1.02 \pm 0.02(stat) \pm 0.06(syst)$, compatible with the one found at 158 GeV per nucleon, has been obtained.

5.4. Energy dependence of charged particle production

In order to examine the energy dependence of charged particle production and to compare our results with the ones obtained for other colliding systems, we study the charged particle pseudorapidity density at midrapidity per participant pair. The results are plotted in figure 6 as a function of $N_{\rm part}$ (evaluated with Glauber calculations). The error bars take into account the statistical error on $dN/d\eta\mid_{\rm max}$ as well as the uncertainty on $<N_{\rm part}>$, while the 8% (resp. 10% at 40 GeV) systematic error on the multiplicity evaluation is not included.

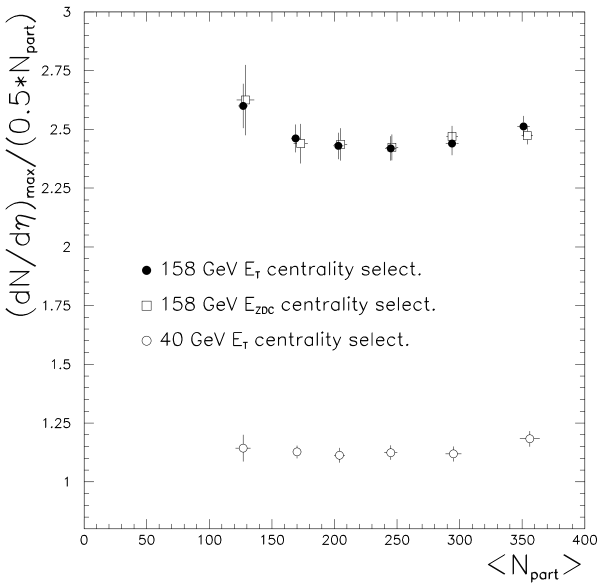

Figure 6. Pseudorapidity density of $N_{\rm ch}$ at midrapidity per participant pair as a function of the number of participants $N_{\rm part}$ in 158 and 40 GeV/nucleon Pb–Pb collisions.

In particular, at 158 GeV per nucleon for the 0-5 % centrality range we obtain:

$$\left(\frac{dN_{ch}/d\eta\mid_{max}}{0.5\cdot < N_{part} >}\right) = 2.49 \pm 0.03(stat) \pm 0.20(syst)$$

which is the average of the values obtained with the $E_{\rm T}$ and $E_{\rm ZDC}$ centrality selections. The systematic error accounts for the 8% systematic uncertainty on the multiplicity evaluation.

At 40 GeV per nucleon, for the 0-5 % centrality range we obtain:

$$\left(\frac{dN_{ch}/d\eta\mid_{max}}{0.5\cdot < N_{part} >}\right) = 1.18 \pm 0.03(stat) \pm 0.17(syst)$$

The large systematic error is due both to the 10% systematic error on the multiplicity and to the uncertainty ($\approx$ 10%) on the evaluation of $<N_{\rm part}>$ for the most central band.

The yield per participant pair thus obtained can be compared to the ones measured at higher energies by RHIC experiments PHOBOS [8, 9, 10] and BRAHMS [11, 12]. Since RHIC measurements are performed in the center-of-mass frame, to make a quantitative comparison we need to convert our results, obtained in the laboratory frame, to the center-of-mass frame. For our data at 158 GeV, assuming pions, kaons and protons relative yields as measured by NA49 [13, 14] and using the formula:

$$\frac{dN_{ch}}{d\mathbf{p}_T d\eta} = \sqrt{1 - \frac{m^2}{m_T^2 \cosh^2 y}}\,\frac{dN_{ch}}{d\mathbf{p}_T dy}$$

the measured yield of 2.49 translates into 2.14 ± 0.17. At 40 GeV we use the relative yields as obtained with VENUS 4.12 since the proton fraction has not been yet measured. We estimate that the measured yield of 1.18 translates into 0.97 ± 0.14 in the center-of-mass frame. In figure 7, the pseudorapidity density per participant pair in the center-of-mass frame for the most central ion-ion collision at SPS and RHIC is shown together with some fits to $p\bar{p}$ data.

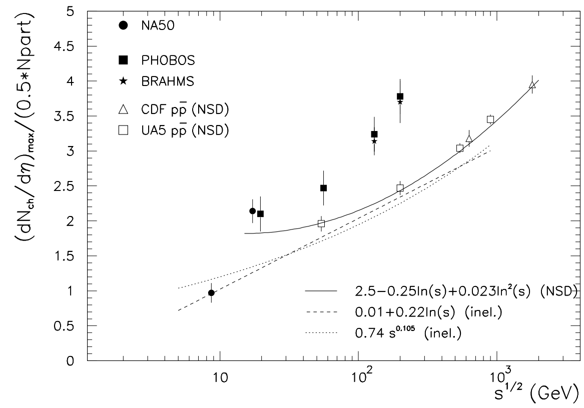

Figure 7. Energy dependence of the pseudorapidity density per participant pair (in the center-of-mass frame) for the most central ion-ion collisions at SPS and RHIC. Fits to $p\bar{p}$ data are superimposed.

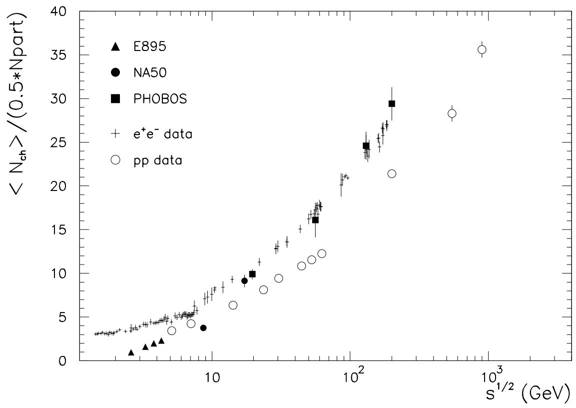

Figure 8. Total charged multiplicity for pp, $p\overline{p}$, e^+e^- and central heavy ion collisions at AGS, SPS and RHIC as a function of $\sqrt{s}$.

When comparing our results with the charged particle pseudorapidity density measured in nucleon-nucleon collisions we observe that our result at 40 GeV/nucleon is in agreement with the fit to data of inelastic $p\overline{p}$ interactions obtained by the UA5 experiment [15] assuming a logarithmic energy dependence, $dN/d\eta\ |_{\max} = (0.01 \pm 0.14) + (0.22 \pm 0.02) \cdot \ln s$. It is also compatible with the UA5 fit obtained assuming a power law energy dependence, $dN/d\eta\ |_{\max} = (0.74 \pm 0.04) \cdot s^{(0.105 \pm 0.006)}$. Therefore, we can conclude that the charged particle yield per participant pair at 40 GeV/nucleon is compatible with the one observed in nucleon-nucleon interactions at similar energies.

On the contrary our result at 158 GeV/nucleon (which is consistent with PHOBOS measurement at $\sqrt{s} = 19.6$ GeV) is more than 50% higher than any of the mentioned fits for the corresponding center-of-mass energy. In addition our result at 158 GeV is also $\sim 20\%$ higher than the fit ($dN/d\eta\ |_{\max} = 2.5 - 0.25 \ln s + 0.023 \ln^2 s$) of the yield obtained by CDF [16] in $p\overline{p}$ non single diffractive interactions for much higher energies. The isospin effect ($\sim 10\%$ among pp, pn and nn interactions [17]) can not account for such a discrepancy.

This comparison suggests a steep increase of particle production in central ion-ion collisions between 40 GeV and 158 GeV which cannot be described by a simple energy scaling as observed in nucleon-nucleon collisions. Therefore, the particle production at 158 GeV/nucleon, although it scales approximately linearly with the number of participants, cannot be explained as an ordinary superposition of nucleon-nucleon interactions.

The total yields of charged particles ($N_{\rm ch}$) in the full phase space for our most central class of events at the two beam energies have been obtained by integrating over η the gaussian fitting functions to the charged particle pseudorapidity distributions. In figure 8, the total charged multiplicity per participant pair in Pb–Pb collisons is shown as a function of $\sqrt{s}$ and it is compared to heavy-ion data from AGS and RHIC as well as to e^+e^- and pp / $p\overline{p}$ results (taken from [18]). It can be observed that the pp / $p\overline{p}$ data show the same energy trend as e^+e^- over the whole energy range. The fact that pp multiplicities lie about 30% below the e^+e^- data at the same energy can be understood in terms of the "leading particle effect" which reduces the effective energy available for particle production in pp collisions. Heavy ion data does not follow the e^+e^- trend over the whole $\sqrt{s}$ range. Instead, they lie below the pp data at AGS energies, cross through the pp data around $\sqrt{s} \sim 10$ GeV and then gradually join the e^+e^- trend above the SPS energies. At RHIC energies, the multiplicity per participant pair in heavy-ion collisions scales in a similar way as e^+e^- data at the same $\sqrt{s}$, suggesting a substantially reduced leading particle effect in central collisions of heavy nuclei at high energy [19].

6. Conclusions

The charged particle pseudorapidity distributions ($dN_{\mathrm{ch}}/d\eta$) in Pb-Pb collisions at 158 GeV per nucleon ($\sqrt{s}$=17.3 GeV) and 40 GeV per nucleon ($\sqrt{s}$=8.77 GeV) beam energy have been measured in six centrality classes defined in terms of fractions of the total inelastic cross-section. The $dN_{\mathrm{ch}}/d\eta$ distributions have been studied as a function of the number of participant nucleons N_{part} and of binary nucleon-nucleon collisions N_{coll} at the two beam energies.

The maximum of the $dN_{\mathrm{ch}}/d\eta$ distributions has been estimated by means of Gaussian fits. The results obtained indicate a steep increase of particle production at SPS energies, which amounts to approximately a factor of two when going from $\sqrt{s} = 8.77$ GeV to 17.3 GeV.

The charged particle pseudorapidity density at midrapidity scales as ${N_{\mathrm{part}}}^{\alpha}$ with $\alpha = 1.00 \pm 0.01(stat) \pm 0.04(syst)$ at 158 GeV per nucleon beam energy, in agreement with the Wounded Nucleon Model predictions. The presence of a contribution scaling like N_{coll} is not observed, so that hard processes seem to play a negligible role in charged particle production at 158 GeV per nucleon. This is also supported by the fact that the value of the α exponent is compatible with the one obtained from the data at 40 GeV per nucleon ($\alpha = 1.02 \pm 0.02(stat) \pm 0.06(syst)$) where no contribution from hard processes is expected.

The increase of charged particle production at midrapidity between 40 and 158 GeV/nucleon can not be described by the simple energy scaling observed in nucleon-nucleon collisions at similar energies.

References

[1] Abreu M C et al. 2002 *Phys. Lett.* B **530** 33
[2] Abreu M C et al. 1997*Phys.Lett.* B **410** 327
[3] Abreu M C et al. 2002 *Phys. Lett.* B **530** 43
[4] Alessandro B et al. 1995 *Nucl.Inst.Meth.* A **360** 189
[5] Alessandro B et al. 2002 *Nucl.Inst.Meth.* A **493** 30
[6] Senger P and Ströbele H 1999 *J. Phys.* G **25** R59
[7] Orear J 1982 *Am. J. Phys.* **50** 912 and Erratum, 1984 *Am. J. Phys.* **52** 278
[8] Back B B et al. 2000 *Phys. Rev. Lett.* **85** 3100
[9] Back B B et al. 2002 *Phys. Rev. Lett.* **88** 022302
[10] Back B B et al. 2003 *Nucl. Phys.* A **715** 490
[11] Bearden I G et al. 2001 *Phys. Lett.* B**523** 227
[12] Bearden I G et al. 2002 *Phys. Rev. Lett.* **88** 202301
[13] Bächler J et al. 1999 *Nucl. Phys.* A **661** 45c
[14] Appelshäuser H et al. 1999 *Phys. Rev. Lett.* **82** 2471
[15] Alner G J et al. 1986 *Z. Phys.* **C 33** 1
[16] Abe F et al. 1990 *Phys. Rev.* **D 41** 2330
[17] Gazdzicki M and Hansen O 1991 *Nucl. Phys.* **A 528** 754
[18] Groom D E et al. 2000 *Eur. Phys. J.* **C 15** 1
[19] Back B B et al. 2003 nucl-ex/0301017 v1